APPLIED AND ENVIRONMENTAL MICROBIOLOGY, Mar. 2006, p. 2005–2013 Vol. 72, No. 3
0099-2240/06/$08.00+0 doi:10.1128/AEM.72.3.2005–2013.2006

A Three-Dimensional Computer Model of Four Hypothetical Mechanisms Protecting Biofilms from Antimicrobials

Jason D. Chambless, Stephen M. Hunt, and Philip S. Stewart*

Center for Biofilm Engineering and Department of Chemical and Biological Engineering, Montana State University—Bozeman, Bozeman, Montana 59717-3980

Received 31 August 2005/Accepted 29 November 2005

Four hypothetical mechanisms for protection of biofilms against antimicrobials were incorporated into a three-dimensional model of biofilm growth and development. The model integrated processes of substrate utilization, diffusion, growth, cell migration, death, and detachment in a cellular automaton framework. Compared to simulations of unprotected biofilms, each of the protective mechanisms provided some tolerance to antimicrobial action. When the mechanisms were compared to each other, the behaviors of the four protective mechanisms produced distinct shapes of killing curves, nonuniform spatial patterns of survival and cell type distribution, and anticipated susceptibility patterns for dispersed biofilm cells. The differences between the protective mechanisms predicted in these simulations could guide the design of experiments to discriminate antimicrobial tolerance mechanisms in biofilms. Each of the mechanisms could be a plausible avenue of biofilm protection.

Microorganisms within biofilms have a remarkable tolerance to killing by antimicrobial agents (26, 39). The reduced susceptibility of bacteria and yeast in biofilms is recognized as an important factor in the persistence of some chronic infections and the troublesome recurrence of fouling in industrial systems. While the reduced antimicrobial and biocide susceptibility in biofilms is well documented, the mechanisms of resistance are incompletely understood (26, 39, 41). Four leading hypotheses explaining the reduced susceptibility of biofilms, diagrammed in Fig. 1, are poor antimicrobial penetration, deployment of adaptive stress responses, physiological heterogeneity in the biofilm population, and the presence of phenotypic variants or persister cells (6, 12, 25, 38). It seems likely that a combination of these factors determines the overall protection in the biofilm (38, 39).

There have been a handful of papers describing neutralization of an antimicrobial agent by a reaction as it diffuses into a biofilm (1, 42). The biofilm is said to consume the antimicrobial agent in the same manner that it would consume a substrate. This consumption could allow biofilms to decrease the concentration of an antimicrobial to a level that would be ineffective in the deeper regions of the biofilm. However, such a protective mechanism would be expected to be present only in thicker biofilms. Also, antimicrobial agents that do not react with or bind to a biofilm can be expected to penetrate in a matter of seconds or minutes (37). Examples of several antimicrobial agents that penetrate biofilms but fail to kill the sessile microorganisms at the rate observed for their planktonic counterparts are plentiful (1, 7, 10, 17, 33, 43, 49).

Bacteria are equipped with a host of stress responses that allow them to cope with environmental adversity. It is possible that the same protective mechanisms are utilized by biofilms. The most compelling version of this second mechanism of biofilm protection is that stress response defenses are induced in biofilm bacteria when they face an environmental challenge, just as they are in bacteria in aqueous suspension. The difference between free-floating cells and biofilm-embedded cells is that the biofilm bacteria are sufficiently protected by other defenses, such as retarded antimicrobial penetration or slow growth, which allows the biofilm cells to respond to an antimicrobial challenge that overwhelms planktonic cells. An example of a stress response that is of obvious interest in the context of antimicrobials is the expression of drug efflux pumps.

The possibility that substrate limitation within a biofilm creates regions of inactive and less susceptible cells remains an attractive explanation for the recalcitrance of biofilms to antimicrobial agents (3, 6, 19, 20). It is clear that there are substrate concentration gradients within biofilms (13, 48). These concentration gradients give rise to corresponding gradients in the microbial growth rate and activity, as observed by researchers using fluorescent probes and reporter genes (35, 45, 46). Since antimicrobials are thought to be more effective in killing actively growing cells, it seems reasonable that in substrate-limited regions of a biofilm the microorganisms could better tolerate the presence of an antimicrobial agent by virtue of their inactivity. However, one would expect that as growing cells within the biofilm are killed, substrate would penetrate into regions that were previously substrate depleted. Thus, dormant microorganisms might lose their tolerance for the antimicrobial agent as substrate becomes available.

A fourth mechanism of antimicrobial resistance in biofilms invokes the possibility of a unique and highly protected phenotypic state that is adopted by a subpopulation of microorganisms in a biofilm (26, 41). This is conceptualized as true differentiation of the cells akin to spore formation that requires the expression of specific sets of genes. Cells in this special state have been termed persisters. Such a phenotypic state is suggested by experiments with young biofilms that display resistance even though they are too thin to pose a

* Corresponding author. Mailing address: Center for Biofilm Engineering and Department of Chemical and Biological Engineering, Montana State University—Bozeman, Bozeman, MT 59717-3980. Phone: (406) 994-1960. Fax: (406) 994-6098. E-mail: phil_s@erc.montana.edu.

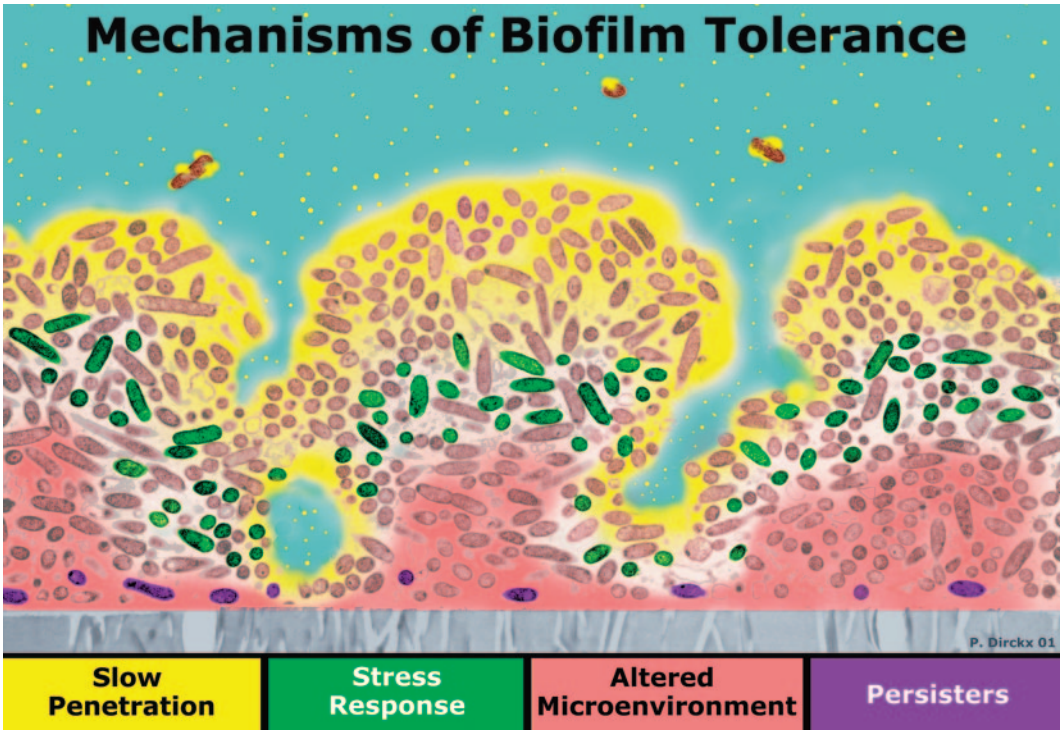

FIG. 1. Four possible mechanisms of biofilm antibiotic resistance. The image is a cross section of a biofilm with the attachment surface (gray) at the bottom and the aqueous phase containing the antibiotic (yellow) at the top. In zones where there is nutrient depletion (red), antibiotic action may be antagonized. Some bacteria may activate stress responses (green), while others may differentiate into a protected phenotype (purple).

barrier to the penetration of either an antimicrobial agent or metabolic substrates (7, 11). Another indication that biofilms may harbor a subpopulation of resistant cells comes from experiments in which most, but not all, of the biofilm is rapidly killed by an antimicrobial (2, 5, 21). The survivors, which may be 1% or less of the original population, persist despite continued exposure to the antimicrobial (2, 34).

Computer models of biofilm dynamics complement experimental investigations and thus are valuable tools in the exploration of biofilm phenomena. Models can be used to test conjectures or make predictions about how specific processes affect biofilm structure or function. Theoretical explorations are particularly attractive because often there are multiple mechanisms that are difficult to separate experimentally. We have been interested in using biofilm models to explore the degrees of protection from killing by antimicrobials that can be conferred by specific tolerance mechanisms. Several previous studies have described biofilm models that incorporate antimicrobial action (8, 14, 15, 23, 28, 36, 40, 44). Using a three-dimensional computer model of biofilm dynamics, we investigated the levels of protection against antimicrobials provided by each of four hypothesized protective mechanisms. The purpose of this study was to characterize the predicted features of four different protective mechanisms when they were incorporated into a multidimensional computer model of biofilm dynamics. In particular, we sought to examine population survival versus antimicrobial exposure time and the spatial patterns of chemical species and cell types within biofilms during or after antimicrobial treatment.

MATERIALS AND METHODS

BacLAB, the computer model used in this study, has been described in detail elsewhere (22). This model uses a hybrid modeling approach in which all soluble components are modeled using discretized differential equations while the individual microorganisms that compose the biofilm are modeled discretely using a cellular automaton algorithm. A cellular automaton is an independent unit, here equated to a bacterial cell, that follows certain behavioral rules. The resulting aggregate behavior of the biofilm therefore emerges from the local interactions between the individual bacteria. The cellular automaton model produces realistic, structurally heterogeneous biofilms (4, 9, 18, 24, 28, 29, 30, 47). Furthermore, it allows the artificial biofilm structure to evolve as a self-organizing process, emulating how bacterial cells organize themselves into biofilms. Two advantages of the hybrid approach are the ability to separate different biofilm processes according to the natural time scale and the fact that the aggregate behavior of the biofilm emerges from the local interactions between individual microorganisms. Some of the processes simulated by the computer model include diffusion of soluble components into the biofilm, substrate and antimicrobial consumption, microbial growth, and biofilm detachment resulting from nutrient starvation. Parameter values are summarized in Table 1, and a representation of a typical BacLAB biofilm simulation is shown in Fig. 2.

The following two sets of simulations were performed for each of the four protective mechanisms: (i) protected with a continuous antimicrobial treatment initiated at hour 100 and lasting 50 h and (ii) unprotected with a continuous antimicrobial treatment initiated at hour 100 and lasting 50 h.

For all unprotected studies the probability of killing due to the presence of the antimicrobial agent was 0.6838 for a 1-h interval. This value was calculated to provide a 6-log reduction in nongrowing suspended cell cultures in a 12-h treatment period by solving the following equality: $(1 - P)^{12} = 10^{-6}$, where P is the probability of killing. Therefore, the probability that a cell will survive a 12-h treatment is 1 in 10^6. At each time that the antimicrobial agent is present, every cell in the simulation generates a random number from a uniform distribution on the interval [0, 1]. If the random number is less than or equal to the probability of killing (0.6838), the cell dies and remains

TABLE 1. Summary of parameters used in the BacLAB model

Parameter	Symbol	Value	Units
Maximum specific growth rate	$\mu_{S,max}$	0.3	h^{-1}
Time step	Δt	1.0	h
Bulk substrate concn	$C_{S,bulk}$	8.0	g m^{-3}
Diffusivity of substrate in the aqueous phase (including the liquid, channels, and voids)	$D_{S,aq}$	7.20×10^{-6}	m^2 h^{-1}
Relative effective diffusivity of substrate in biofilm	$D_{S,e}/D_{S,aq}$	0.55	
Local nutrient concn threshold	$C_{S,min}$	1.0	g m^{-3}
Substrate Monod half-saturation coefficient	K_S	0.1	g m^{-3}
Avg cell mass	m_{avg}	1.75×10^{-13}	g
No. of initial colonies	N_c	28	
No. of nodes in x direction	N_x	300	
No. of nodes in y direction	N_y	300	
Radius of initial colonies	R_c	8.55×10^{-6}	m
Duration of time below $C_{S,min}$ before detachment	t_{detach}	24	h
Biomass yield (g_X) per gram of substrate (g_S)	Y_{XS}	0.24	g_X g_S^{-1}

metabolically inactive for the remainder of the simulation or until it detaches from the biofilm. If the random number is greater than 0.6838, the cell continues to function normally.

The slow penetration, stress response, and persister mechanisms use the same probability for killing of live cells that is found in the unprotected simulations. In order to provide a form of protection, the slow penetration and stress response mechanisms include restrictions on when this probability equation is active as a result of the barrier to antimicrobial diffusion. For the persister mechanism, no restrictions are placed on this probability since the protection stems from the inclusion of the spore-like persister cells. The substrate limitation mechanism is different from each of these mechanisms and the unprotected simulations in that the probability of killing is altered so that it is directly proportional to the local substrate concentration.

In the simulations in which the slow penetration mechanism is active, both live and dead biofilm cells consume the antimicrobial as it diffuses into the biofilm. The parameters for antimicrobial diffusion and consumption are shown in Table 2.

In the aqueous environment modeled here, the bulk liquid is well mixed but imposes no shear stress on the biofilm. The antimicrobial is transported solely by diffusion in the biofilm. The local concentrations are a result of molecular diffusion and reaction (consumption or production) with the bacteria. The diffusional time constant is approximately 100 orders of magnitude smaller than that for bacterial cell division (28). Thus, molecular diffusion can be assumed to be at a steady state with respect to the bacterial growth.

Since the antimicrobial is steadily depleted, there is an antimicrobial concentration at which it is no longer effective against the biofilm cells. This concentration, otherwise known as the MIC, is set at 1.0 g m^{-3}. It follows that as the

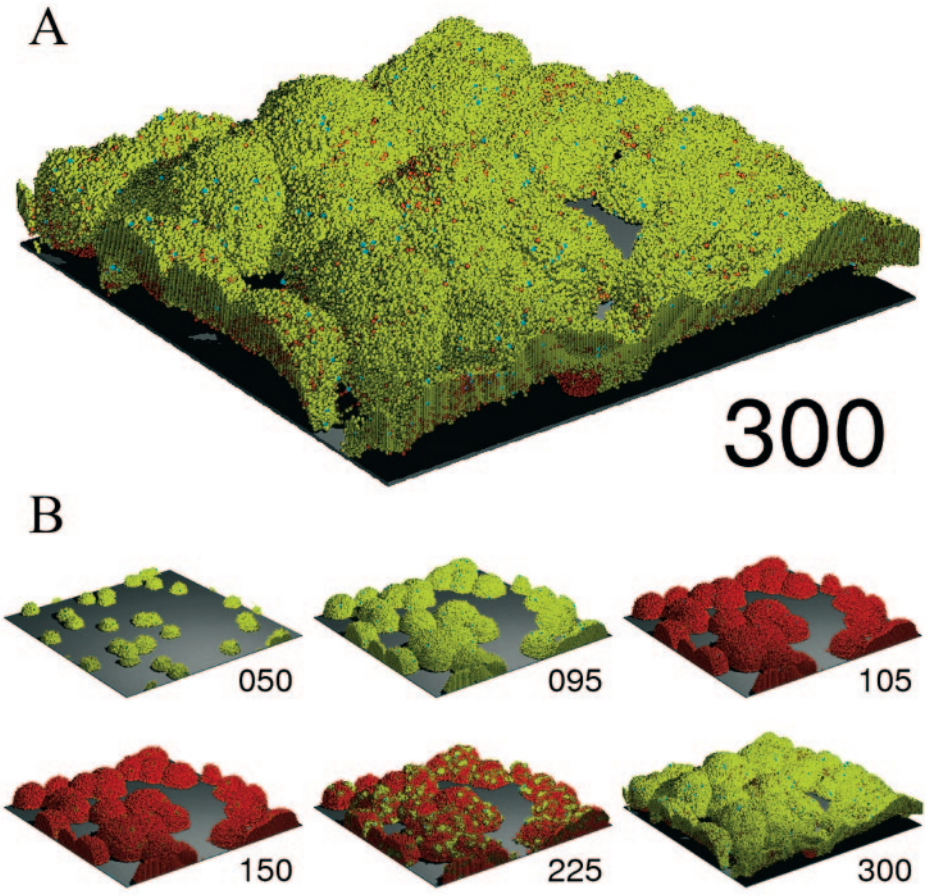

FIG. 2. Three-dimensional representation of the BacLAB model, showing a biofilm with live (green), dead (red), and persister (blue) cells at hour 300 (150 h after completion of a 50-h antimicrobial treatment) (A) and during a 300-h simulation in which the persister protection mechanism is active (B). Biofilm formation begins with the development of independent cell clusters that merge over time. Antimicrobial treatment initiated at 100 h rapidly kills most of the live cells, but persister cells survive. When persister cells eventually resuscitate, they give rise to new growth that begins in clonal pockets but rapidly extends throughout the biofilm. A video of this simulation can be viewed at www.erc.montana.edu/Res-Lib99-SW/Movies/Database/MD_DisplayScript.asp.

TABLE 2. BacLAB parameters for use in antimicrobial diffusion and consumption

Parameter	Symbol	Value	Units
Maximum specific reaction rate of antimicrobial	$k_{A,\max}$	2.5	$g_A\ g_S^{-1}\ h^{-1}$
Bulk antimicrobial concn	$C_{A,\text{bulk}}$	10.0	$g\ m^{-3}$
Diffusivity of the antimicrobial in the aqueous phase (including the liquid, channels, and voids)	$D_{A,\text{aq}}$	1.44×10^{-6}	$m^2\ h^{-1}$
Relative effective diffusivity of the antimicrobial in biofilm	$D_{A,e}/D_{A,\text{aq}}$	0.25	
Antibiotic Monod half-saturation coefficient	K_A	1.0	$g\ m^{-3}$

TABLE 3. Log reductions for live cells for each protective mechanism after a 50-h antimicrobial treatment

Simulation	Slow penetration[a]	Adaptation	Substrate limitation	Persisters
1	>5.93	1.59	0.59	5.93
2	>5.91	1.56	0.68	5.92
3	>5.89	1.50	0.57	5.90
4	>5.93	1.41	0.75	5.86
5	>5.93	1.54	0.51	5.30
6	>5.93	1.57	0.54	5.92
Avg	>5.92	1.53	0.61	5.80
SD		0.06	0.09	0.25

[a] No live cells remained at the end of the antimicrobial treatment in each of the slow penetration simulations.

thickness of a biofilm increases, so too does the chance of thwarting an antimicrobial challenge.

The stress response mechanism includes the same rules that are used for slow penetration protection, diffusion and consumption of the antimicrobial based on the parameters shown in Table 2, and no killing below an MIC of 1.0 g m^{-3}, but with one variation: if the antimicrobial concentration is greater than or equal to one-tenth the MIC and the cell has not been killed by the antimicrobial, then the cell has some probability of switching to an adapted state. This probability is 0.06838, 10% of the probability of death. In the adapted state the cell acquires absolute resistance to the effects of the antimicrobial and continues its cellular functions uninhibited by the antimicrobial.

For the substrate limitation mechanism, the antimicrobial efficacy was simulated to be proportional to the amount of substrate available to the microorganism; that is, $P = (P_{\text{MAX}}/C_{S0}) \cdot C_S$, where P_{MAX} is the maximum probability of killing and is equal to the probability of killing used in the base case simulations, C_{S0} is the substrate concentration in the bulk fluid, and C_S is the local substrate concentration at a particular cell. Thus, cells in substrate-rich regions of the biofilm have the lowest antimicrobial tolerance, whereas cells in substrate-depleted regions are expected to be tolerant to antimicrobial killing.

When the persister mechanism is simulated, the protection stems from the random conversion of live cells to persister cells. Persister cells are nongrowing, spore-like cells that are nearly impervious to antimicrobial effects. Persisters are constantly being formed, with no regard to the presence of an antimicrobial. The probability of a live cell converting to a persister cell is 0.0015, and the probability of a persister cell converting back to a live cell is 0.15. These values were chosen to yield a persister population that is approximately 1% of the total population. The probability that a persister cell will be killed by an antimicrobial is 0.0034, which makes such a cell 200-fold more resistant to the antimicrobial than a normal live cell.

We did not conduct a full analysis of the sensitivity of the model to the values of key parameters. Rather, it was our intent to illustrate the qualitative behaviors predicted when certain biological and physical phenomena were simulated.

All simulations progressed through a 300-h experiment, including 100 h of initial attachment and unchallenged growth, 50 h of antimicrobial treatment, and 150 h of recovery.

RESULTS AND DISCUSSION

The computer model used in this investigation simulated biofilm development over 300 h, along with the response to a 50-h continuous antimicrobial treatment for both unprotected and protected biofilms. Because there are stochastic components of the model, the simulation results varied slightly from run to run even when the same parameter settings and initial conditions were used. We therefore ran each simulation case six times.

We selected a value for the antimicrobial killing rate that corresponded to a 6-log reduction in the number of viable cells after 12 h of exposure of planktonic cells to the antimicrobial agent in the absence of cell growth. Even with the inclusion of biofilm growth during an antimicrobial treatment, we anticipated that each of the unprotected biofilms would be eradicated by a 50-h treatment. In all cases, this was indeed the result. All of the unprotected biofilms were killed completely by hour 15 of the antimicrobial treatment.

For the protected biofilms, Table 3 summarizes the log reductions produced by the 50-h antimicrobial treatment.

Slow penetration. The killing curve for the slow penetration investigations and the corresponding base case simulations are shown in Fig. 3. The survival curve is highly nonlinear. Retarded antimicrobial penetration provided good protection to the biofilm up until around 15 h after the onset of treatment. If the treatment had been a 12-h treatment, the biofilm would have easily survived due to the protection of slow penetration. After this time, however, viability decreased sharply as the diffusion of the antimicrobial outpaced the neutralization by the bacteria. This imbalance led to complete disinfection of the biofilm colony 15 to 20 h before the end of the 50-h treatment.

When the slow penetration mechanism is active, both live and dead biofilm cells consume the antimicrobial. The effects of this consumption are evident in the profile of the antimicrobial concentration in the biofilm 10 h after the treatment

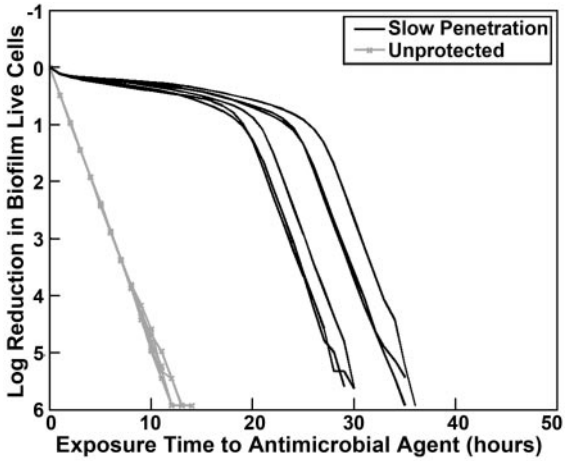

FIG. 3. Log reduction in biofilm live cells during a 50-h antimicrobial treatment for unprotected biofilms and biofilms protected by the slow penetration mechanism. The biofilms without protection are completely eradicated after 13 h, while the protected biofilms are able to withstand the antimicrobial for 30 to 35 h.

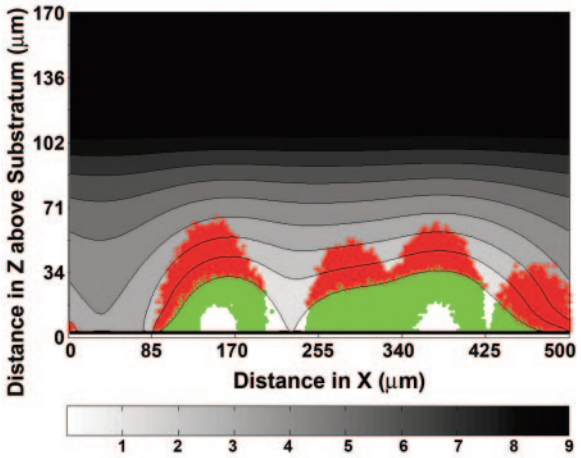

FIG. 4. Concentration profile for the antimicrobial in a slow penetration simulation after hour 110, 10 h after introduction of the antimicrobial. The image is a two-dimensional cross section of the biofilm with the substratum at the bottom and the bulk fluid at the top. The isoline indicates antimicrobial concentrations (in g m^{-3}). The figure shows that there is a clear separation of live (green) and dead (red) cells at an antimicrobial concentration of 1.0 g m^{-3}. The antimicrobial concentration used was 10 g m^{-3}; this concentration occurs above the domain plotted.

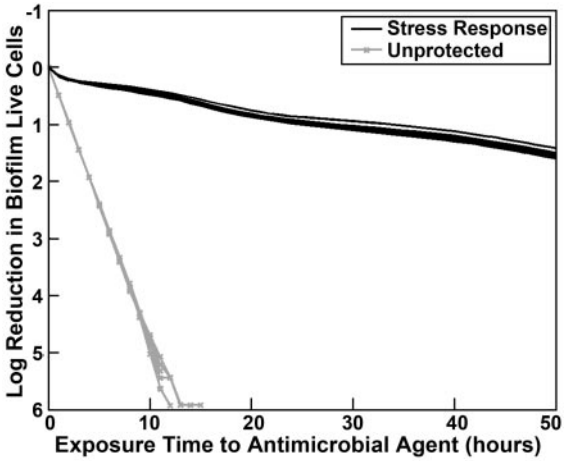

FIG. 5. Log reduction in biofilm live cells during a 50-h antimicrobial treatment for unprotected biofilms and biofilms protected by the stress response and slow penetration mechanisms. The biofilms without protection are completely eradicated after 15 h, while the protected biofilms are able to withstand the antimicrobial throughout the treatment time with an average log reduction of 1.53 ± 0.06.

began, as shown in Fig. 4. The concentration of antimicrobial agent is reduced in and around the biofilm clusters, even in the fluid, where there is no consumption of the antimicrobial. This is because the stagnant fluid outside the biofilm provides resistance to diffusive mass transfer. There are bands of live cells at the bottoms of the larger biofilm clusters, where the antimicrobial concentration is less than 10% of the bulk concentration. The separation between live and dead cells is distinct as there are few live cells at concentrations above 1.0 g m^{-3} and almost no dead cells at concentrations below this concentration.

The results of these simulations are most likely highly dependent on the choice of parameter values (Table 2). If the antibiotic consumption rate were increased, the biofilm would stand a greater chance of surviving the treatment. There seems to be a critical consumption rate that, once passed, allows the biofilm to consume the antimicrobial quickly enough that no investigation would reveal eradication of the biofilm. This assumption was not tested in this study. This concept has been discussed in previous studies of beta-lactam penetration (14, 27).

It is interesting to consider the fate of a biofilm that is disaggregated and then exposed to an antimicrobial agent. In the case of the slow penetration mechanism, the inherent susceptibility of all the cells in a biofilm is identical to that of their planktonic counterparts. The only difference is that the antimicrobial concentrations experienced by the biofilm population are heterogeneous and lower than those experienced by a planktonic population. If slow penetration is the sole basis for biofilm tolerance, we would anticipate that dispersal of a biofilm would immediately and completely restore its full planktonic susceptibility. This behavior has been reported in some studies (2, 16, 42, 45).

Stress response. When slow penetration is combined with an adaptive stress response, greater protection is predicted by the model (compare Fig. 5 to Fig. 3). In this case, the antimicrobial fails to eradicate the biofilm. This is due to the transformation of live cells into adapted cells, which are immune to the antimicrobial agent. The adapted cells continue to grow and outcompete other cell types in the antimicrobial-treated biofilm community. By the end of the simulation, there are no nonadapted live cells remaining.

It is evident from the representative antimicrobial concentration profile shown in Fig. 6 that incomplete penetration of the antimicrobial limits killing to the uppermost layers of the biofilm. There is a sharp delineation between live and dead

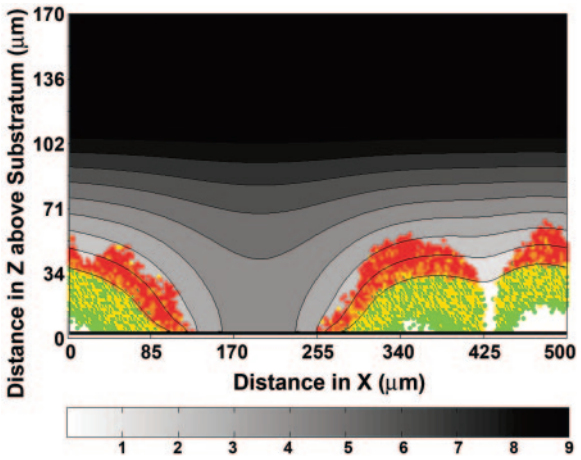

FIG. 6. Concentration profile for the antimicrobial in a stress response simulation after hour 110, 10 h after introduction of the antimicrobial. The image is a two-dimensional cross section of the biofilm with the substratum at the bottom and the bulk fluid at the top. The isoline indicates antimicrobial concentrations (in g m^{-3}). The antimicrobial concentration used was 10 g m^{-3}; this concentration occurs above the domain plotted. A small band containing only live cells is also evident near the bottom of the biofilm. In this area the antimicrobial concentration is less than 0.1 g m^{-3}. Above this band, adaptive cells (yellow) are formed.

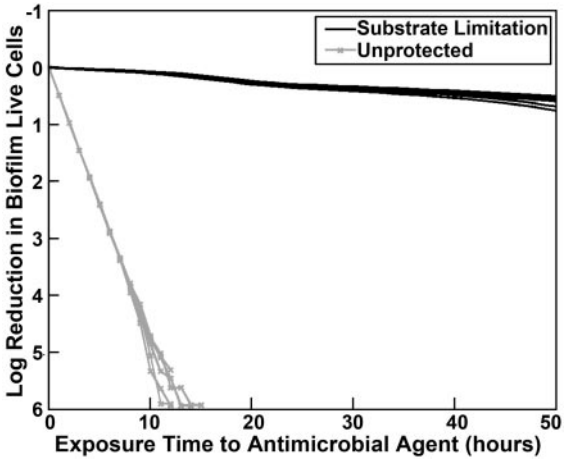

FIG. 7. Log reduction in biofilm live cells during a 50-h antimicrobial treatment for unprotected biofilms and biofilms protected by the substrate limitation mechanism. The biofilms without protection are completely eradicated after 15 h, while the protected biofilms are able to withstand the antimicrobial throughout the treatment time with an average log reduction of 0.61 ± 0.09.

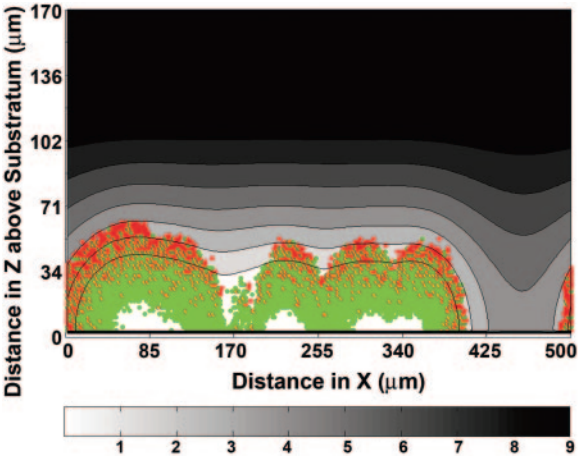

FIG. 8. Concentration profile for the substrate in a substrate limitation simulation after hour 110, 10 h after introduction of the antimicrobial. The image is a two-dimensional cross section of the biofilm with the substratum at the bottom and the bulk fluid at the top. The isoline indicates substrate concentrations (in g m^{-3}). The majority of dead cells (red) are concentrated at the top of the biofilm, where the local maximum substrate concentration occurs. Few dead cells are found deep within the biofilm, where the local substrate concentration can fall below 0.1 g m^{-3}. The substrate concentration used was 10 g m^{-3}; this concentration occurs above the domain plotted.

cells corresponding to the isoline of antimicrobial concentration equal to 1.0 g m^{-3}. The antimicrobial concentration gradient allows cells in the lower regions of the biofilm to adapt and convert from the live cell state to the adapted cell state (Fig. 6). This transformation occurs with a fixed probability wherever the antimicrobial concentration is greater than 0.1 g m^{-3}.

The outcome simulated here is dependent on the choice of parameter values (Table 2). The threshold concentration for implementation of the stress response (0.1 g m^{-3} in this study) is critical. When this value is less than the concentration required for killing, then there is a window of antimicrobial concentrations (0.1 to 1.0 g m^{-3} in this study) at which adaptation is relatively favorable. Note that adaptation can still occur at concentrations above the killing threshold concentration, but in this situation there is a race between the transformation of live cells to dead cells (killing) and the transformation of live cells to adapted cells (adaptation). The essential property of the adapted cell state is its invulnerability to killing, which allows such cells, even if only small numbers are generated, to eventually dominate the biofilm population.

One of the predictions implicit in the simulation of the stress response mechanism is that the adapted cells in an antimicrobial-treated biofilm should retain their antimicrobial tolerance for some time even if they are dispersed from the biofilm. Adapted cells may revert to the unadapted state if they are grown in the absence of the antimicrobial agent, but this process presumably requires some time. A biofilm population that is disaggregated and immediately challenged with an antimicrobial agent would be expected to contain some adapted cells and therefore exhibit susceptibility intermediate between that of a normal (unadapted) planktonic population and that of an intact biofilm. This has been observed in some experimental studies (3, 19, 20, 31). While in this investigation we did not incorporate the process of adapted cells returning to an unadapted state, this would be a straightforward modification.

Substrate limitation. When substrate-limited killing is simulated, the biofilm is well protected (Fig. 7). Since cells in the outer layers of the biofilm are killed (Fig. 8) and these dead cells no longer consume substrate, substrate should permeate into the biofilm, feeding the inner layers and making them vulnerable to the action of the antimicrobial. This process is not particularly rapid, as Fig. 7 shows. This result of prolonged tolerance afforded by the substrate limitation mechanism is in agreement with the predictions of a previous study conducted with a one-dimensional biofilm model (32). Note that the simulations and results described here and below do not incorporate the slow penetration protection discussed above.

According to the substrate limitation mechanism, cells in substrate-rich regions of the biofilm have the greatest antimicrobial susceptibility, whereas cells in substrate-depleted regions are expected to be relatively tolerant to antimicrobial killing. This behavior is evident in the substrate concentration profile shown in Fig. 8, which shows the domination of live cells in the innermost, and nutrient-limited, layers of the biofilm. Dead cells are localized preferentially in the surface layers of the biofilm, where substrate concentrations are highest. The stratification of live and dead cells is not as sharp as that predicted by the slow penetration and stress response mechanisms. Surviving cells can be found at the outermost reaches of the biofilm, and dead cells can be found deep in the biofilm interior.

If cells were dispersed from a biofilm protected by substrate limitation, how susceptible would they be to antimicrobial challenge? If the biofilm were dispersed in a substrate-replete medium, the susceptibility should approach that of the typical planktonic state. Awakening from a nongrowing, starved state to a state of rapid growth may require some time, so susceptibility may not be restored instantly. This could explain the occasional observation of intermediate susceptibility of dispersed biofilm cells (3, 19, 20, 31). An interesting experiment

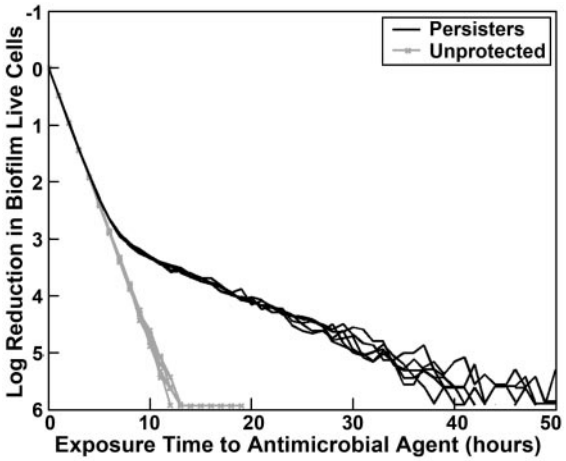

FIG. 9. Log reduction in biofilm live cells during a 50-h antimicrobial treatment for unprotected biofilms and biofilms protected by the persister mechanism. The biofilms without protection are completely eradicated after 11 to 19 h, while the protected biofilms are able to withstand the antimicrobial for 40 to 50 h with an average log reduction of 5.80 ± 0.25.

would be to disperse biofilm cells in a substrate-limited medium (or medium lacking substrate altogether) and then apply an antimicrobial challenge. If substrate limitation is the sole protective mechanism, then these cells should retain the full level of tolerance exhibited by the intact biofilm. There are very few examples of this kind of experiment, and the data are inconclusive.

Persisters. The time course of killing of cells in a biofilm protected by persister formation is distinct from the patterns exhibited by the other three protective mechanisms (Fig. 9). Most of a biofilm consists of cells whose intrinsic susceptibility is the same as that of a planktonic cell. Thus, the majority of the biofilm population is rapidly killed. The persister subpopulation, which constitutes approximately 1% of the biofilm initially, is very slowly killed. The rate of killing of the persister cells is controlled by the slow, random reversion of these cells to the live cell state. As persisters convert to live cells, they become vulnerable to the antimicrobial. This mechanism leads to a bilinear killing curve in which rapid killing of most of the biofilm is followed by very slow killing of the remainder of the population. The noise at the bottom of the curve comes from the stochastic conversion and resuscitation of live and persister cells, respectively.

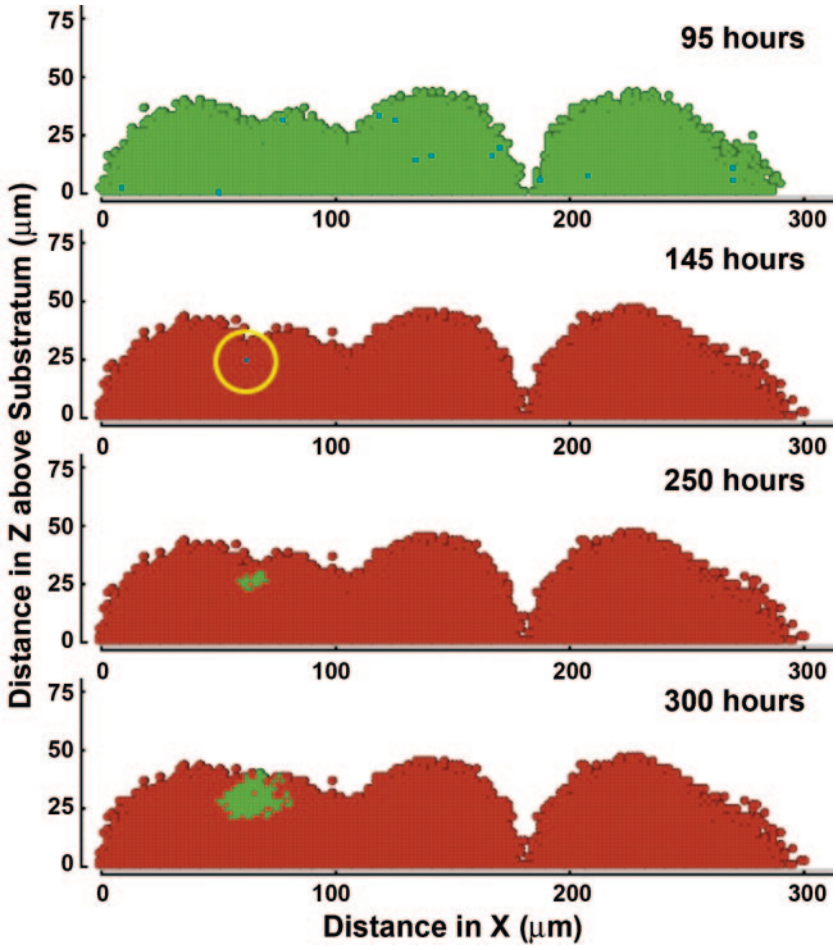

FIG. 10. Cross section of a persister-protected biofilm. The same cross section is shown at 95, 145, 250, and 300 h. The results show that a single persister cell (yellow circle at hour 145) can reseed the colony with new growth after an antimicrobial treatment has ended.

TABLE 4. Characteristics of alternative protective mechanisms

Mechanism	Shape of killing curve	Distribution of cell types	Susceptibility of dispersed cells
Slow penetration	Approximately bilinear, killing accelerating with time	Sharply stratified with dead cells on the outside and live cells inside	Same as planktonic cells
Stress response	Approximately linear	Sharply stratified with dead cells on the outside and live cells inside	Equal to or less than planktonic cells, depending on how fast adapted cells return to an unadapted state
Substrate limitation	Approximately linear	Noisily stratified with dead cells mostly on the outside and live cells mostly inside	Equal to or less than planktonic cells, depending on how fast inactive cells return to an active state
Persisters	Approximately bilinear, killing decelerating with time	Clonal survival of pockets of live cells at random locations within the biofilm	Same as intact biofilm

The pattern of survival and regrowth inside a biofilm protected by persister formation is also distinct from the patterns predicted for the other three protective mechanisms (Fig. 10). Regrowth of the biofilm from isolated persister cells occurs in randomly located clonal pockets. The lone persister in the second panel of Fig. 10 resuscitated to the live cell state and began to grow, effectively reseeding the biofilm. This spatial pattern is qualitatively different from the stratified patterns of killing observed with the other protective mechanisms. It is worth reiterating that this result occurs in an environment free of convective mixing of biomass.

Dispersing cells from a biofilm protected by persister formation should not change the overall susceptibility, unless, of course, there is a period between the dispersal of the biofilm and the application of the antimicrobial that is sufficient to allow reversion of the persister cells to live cells. If the antimicrobial challenge is applied quickly, however, the live cells remain vulnerable and persister cells should remain mostly invulnerable. Thus, the dispersed cells would be expected to exhibit susceptibility similar to that of the intact biofilm. While experimenters rarely analyze the susceptibility of dispersed biofilm cells, when they do, they find that the dispersed cells are usually more susceptible than the intact biofilm.

Conclusions. A three-dimensional computer model of biofilm dynamics has been developed as a tool for investigating mechanisms of protection from antimicrobial agents in biofilms. All four of the hypothetical mechanisms explored in this study provided protection according to model simulations. It is not appropriate to compare the relative degrees of protection afforded by these mechanisms because the results depend on the choice of key parameters whose true values are unknown. What can be compared are the qualitative features of the behaviors predicted by the simulations since these features are relatively insensitive to the choice of specific parameter values. Features that were different in the four protective mechanisms were the shape of the survival-versus-time curve and the spatial patterns of survival and cell type distribution (Table 4).

These results may be helpful in designing laboratory experiments to elucidate protective mechanisms in biofilms. We suggest that the most powerful approach to this problem would be to measure, in the same experimental system, all three of the aspects described in Table 4 (i.e., the shape of killing curves, the spatial pattern of antimicrobial action within the biofilm, and the relative susceptibility of resuspended biofilm cells). Although there are methods for measuring each of these features, we are aware of no single study in which all three have been measured concurrently.

One of the ways in which the work described in this paper differs from previous modeling studies of antimicrobial action against biofilms is in the incorporation of stochastic elements in the model. Processes that have been simulated with random or probabilistic components in the current study include the initial seeding of the substratum, the direction in which biomass is displaced when growth occurs, and the transformation of live cells to dead cells in the presence of an antimicrobial. The result is that no two simulations produce exactly the same quantitative result. The variability between simulations with identical input parameter values captures some of the variation that is measured by experimenters working with real biofilms. The stochastic elements of the model provide the ability to repeat experiments and statistically analyze the results just as an experimenter would in a real-world lab investigation.

ACKNOWLEDGMENT

This work was made possible by grant 5R01GM067245-02 from the National Institutes of Health.

REFERENCES

1. **Anderl, J. N., M. J. Franklin, and P. S. Stewart.** 2000. Role of antibiotic penetration limitation in *Klebsiella pneumoniae* biofilm resistance to ampicillin and ciprofloxacin. Antimicrob. Agents Chemother. **44:**1818–1824.
2. **Anderl, J. N., J. Zahller, F. Roe, and P. S. Stewart.** 2003. Role of nutrient limitation and stationary-phase existence in *Klebsiella pneumoniae* biofilm resistance to ampicillin and ciprofloxacin. Antimicrob. Agents Chemother. **47:**1251–1256.
3. **Baillie, G. S., and L. J. Douglas.** 1998. Effect of growth rate on resistance of *Candida albicans* biofilms to antifungal agents. Antimicrob. Agents Chemother. **42:**1900–1905.
4. **Barker, G. C., and M. J. Grimson.** 1993. A cellular automaton model of microbial growth. Binary **5:**132–137.
5. **Brooun, A., S. Liu, and K. Lewis.** 2000. A dose-response study of antibiotic resistance in *Pseudomonas aeruginosa* biofilms. Antimicrob. Agents Chemother. **44:**640–646.
6. **Brown, M. R., D. G. Allison, and P. Gilbert.** 1988. Resistance of bacterial biofilms to antibiotics: a growth-rate related effect? J. Antimicrob. Chemother. **22:**777–780.
7. **Cochran, W. L., G. A. McFeters, and P. S. Stewart.** 2000. Reduced susceptibility of thin *Pseudomonas aeruginosa* biofilms to hydrogen peroxide and monochloramine. J. Appl. Microbiol. **88:**22–30.
8. **Cogan, N. G., R. Cortez, and L. Fauci.** 2005. Modeling physiological resistance in bacterial biofilms. Bull. Math. Biol. **67:**831–853.
9. **Colasanti, R. L.** 1992. Cellular automata models of microbial colonies. Binary **4:**191–193.
10. **Darouiche, R. O., A. Dhir, A. J. Miller, G. C. Landon, I. I. Raad, and D. M. Musher.** 1994. Vancomycin penetration into biofilm covering infected prostheses and effect on bacteria. J. Infect. Dis. **170:**720–723.
11. **Das, J. R., M. Bhakoo, M. V. Jones, and P. Gilbert.** 1998. Changes in the biocide susceptibility of *Staphylococcus epidermidis* and *Escherichia coli* cells

associated with rapid attachment to plastic surfaces. J. Appl. Microbiol. **84:**852–858.
12. **Davies, D.** 2003. Understanding biofilm resistance to antibacterial agents. Nat. Rev. Drug Discov. **2:**114–122.
13. **de Beer, D., P. Stoodley, F. Roe, and Z. Lewandowski.** 1994. Effects of biofilm structures on oxygen distribution and mass-transport. Biotechnol. Bioeng. **43:**1131–1138.
14. **Dibdin, G. H., S. J. Assinder, W. W. Nichols, and P. A. Lambert.** 1996. Mathematical model of beta-lactam penetration into a biofilm of *Pseudomonas aeruginosa* while undergoing simultaneous inactivation by released beta-lactamases. J. Antimicrob. Chemother. **38:**757–769.
15. **Dodds, M. G., K. J. Grobe, and P. S. Stewart.** 2000. Modeling biofilm antimicrobial resistance. Biotechnol. Bioeng. **68:**456–465.
16. **Duguid, I. G., E. Evans, M. R. Brown, and P. Gilbert.** 1992. Effect of biofilm culture upon the susceptibility of *Staphylococcus epidermidis* to tobramycin. J. Antimicrob. Chemother. **30:**803–810.
17. **Dunne, W. M., E. O. Mason, and S. L. Kaplan.** 1993. Diffusion of rifampin and vancomycin through a *Staphylococcus epidermidis* biofilm. Antimicrob. Agents Chemother. **37:**2522–2526.
18. **Eberl, H. J., C. Picioreanu, J. J. Heijnen, and M. C. M. van Loosdrecht.** 2000. A three-dimensional numerical study on the correlation of spatial structure, hydrodynamic conditions, and mass transfer and conversion in biofilms. Chem. Eng. Sci. **55:**6209–6222.
19. **Evans, D. J., D. G. Allison, M. R. Brown, and P. Gilbert.** 1990. Effect of growth-rate on resistance of gram-negative biofilms to cetrimide. J. Antimicrob. Chemother. **26:**473–478.
20. **Evans, D. J., D. G. Allison, M. R. Brown, and P. Gilbert.** 1991. Susceptibility of *Pseudomonas aeruginosa* and *Escherichia coli* biofilms towards ciprofloxacin: effect of specific growth rate. J. Antimicrob. Chemother. **27:**177–184.
21. **Goto, T., Y. Nakame, M. Nishida, and Y. Ohi.** 1999. In vitro bactericidal activities of beta-lactamases, amikacin, and fluoroquinolones against *Pseudomonas aeruginosa* biofilm in artificial urine. Urology **53:**1058–1062.
22. **Hunt, S. M., M. A. Hamilton, J. T. Sears, G. Harkin, and J. Reno.** 2003. A computer investigation of chemically mediated detachment in bacterial biofilms. Microbiology **149:**1155–1163.
23. **Hunt, S. M., M. A. Hamilton, and P. S. Stewart.** 2005. A 3D model of antimicrobial action on biofilms. Water Sci. Technol. **52:**143–148.
24. **Kreft, J. U., G. Booth, and J. W. T. Wimpenny.** 1998. BacSim, a simulator for individual-based modelling of bacterial colony growth. Microbiology **144:** 3275–3287.
25. **Lewis, K.** 2001. Riddle of biofilm resistance. Antimicrob. Agents Chemother. **45:**999–1007.
26. **Mah, T. C., and G. A. O'Toole.** 2001. Mechanisms of biofilm resistance to antimicrobial agents. Trends Microbiol. **9:**34–39.
27. **Nichols, W. W., M. J. Evans, M. P. E. Slack, and H. L. Walmsley.** 1989. The penetration of antibiotics into aggregates of mucoid and non-mucoid *Pseudomonas aeruginosa*. J. Gen. Microbiol. **135:**1291–1303.
28. **Noguera, D. R., G. Pizarro, D. A. Stahl, and B. E. Rittmann.** 1999. Simulation of multispecies biofilm development in three dimensions. Water Sci. Technol. **39:**123–130.
29. **Picioreanu, C., M. C. M. van Loosdrecht, and J. J. Heijnen.** 1998. A new combined differential-discrete cellular automaton approach for biofilm modeling: application for growth in gel beads. Biotechnol. Bioeng. **57:**718–731.
30. **Picioreanu, C., M. C. M. van Loosdrecht, and J. J. Heijnen.** 1999. Discrete-differential modelling of biofilm structure. Water Sci. Technol. **39:**115–122.
31. **Pyle, B. H., and G. A. McFeters.** 1990. Iodine susceptibility of pseudomonads grown attached to stainless steel surfaces. Biofouling **2:**113–120.
32. **Roberts, M. E., and P. S. Stewart.** 2004. Modeling antibiotic tolerance in biofilms by accounting for nutrient limitation. Antimicrob. Agents Chemother. **48:**48–52.
33. **Shigeta, M., G. Tanaka, H. Komatsuzawa, M. Sugai, H. Suginaka, and T. Usui.** 1997. Permeation of antimicrobial agents through *Pseudomonas aeruginosa* biofilms: a simple method. Chemotherapy **43:**340–345.
34. **Spoering, A. L., and K. Lewis.** 2001. Biofilms and planktonic cells of *Pseudomonas aeruginosa* have similar resistance to killing by antimicrobials. J. Bacteriol. **183:**6746–6751.
35. **Sternberg, C., B. B. Christensen, T. Johansen, A. Toftgaard Nielsen, J. B. Andersen, M. Givskov, and S. Molin.** 1999. Distribution of bacterial growth activity in flow-chamber biofilms. Appl. Environ. Microbiol. **65:**4108–4117.
36. **Stewart, P. S.** 1994. Biofilm accumulation model that predicts antibiotic resistance of *Pseudomonas aeruginosa* biofilms. Antimicrob. Agents Chemother. **38:**1052–1058.
37. **Stewart, P. S.** 1996. Theoretical aspects of antibiotic diffusion into microbial biofilms. Antimicrob. Agents Chemother. **40:**2517–2522.
38. **Stewart, P. S.** 2002. Mechanisms of antibiotic resistance in bacterial biofilms. Int. J. Med. Microbiol. **292:**107–113.
39. **Stewart, P. S., and J. W. Costerton.** 2001. Antibiotic resistance of bacteria in biofilms. Lancet **358:**135–138.
40. **Stewart, P. S., M. A. Hamilton, B. R. Goldstein, and B. T. Schneider.** 1996. Modeling biocide action against biofilms. Biotechnol. Bioeng. **49:**445–455.
41. **Stewart, P. S., G. A. McFeters, and C.-T. Huang.** 2000. Biofilm control by antimicrobial agents, p. 373–405. *In* J. D. Bryers (ed.), Biofilms II. Process analysis and applications. Wiley-Liss, New York, N.Y.
42. **Stewart, P. S., J. Rayner, F. Roe, and W. M. Rees.** 2001. Biofilm penetration and disinfection efficacy of alkaline hypochlorite and chlorosulfamates. J. Appl. Microbiol. **91:**525–532.
43. **Suci, P. A., M. W. Mittelman, F. P. Yu, and G. G. Geesey.** 1994. Investigation of ciprofloxacin penetration into *Pseudomonas aeruginosa* biofilms. Antimicrob. Agents Chemother. **38:**2125–2133.
44. **Szomolay, B., I. Klapper, J. Dockery, and P. S. Stewart.** 2005. Adaptive responses to antimicrobial agents in biofilms. Environ. Microbiol. **7:**1186–1191.
45. **Walters, M. C., III, F. Roe, A. Bugnicourt, M. F. Franklin, and P. S. Stewart.** 2003. Contributions of antibiotic penetration, oxygen limitation, and low metabolic activity to tolerance of *Pseudomonas aeruginosa* biofilms to ciprofloxacin and tobramycin. Antimicrob. Agents Chemother. **47:**317–323.
46. **Wentland, E. J., P. S. Stewart, C. T. Huang, and G. A. McFeters.** 1996. Spatial variations in growth rate within *Klebsiella pneumoniae* colonies and biofilm. Biotechnol. Prog. **12:**316–321.
47. **Wimpenny, J. W. T., and R. Colasanti.** 1997. A unifying hypothesis for the structure of microbial biofilms based on cellular automaton models. FEMS Microbiol. Ecol. **22:**1–16.
48. **Xu, K. D., P. S. Stewart, F. Xia, C. T. Huang, and G. A. McFeters.** 1998. Spatial physiological heterogeneity in *Pseudomonas aeruginosa* biofilm is determined by oxygen availability. Appl. Environ. Microbiol. **64:**4035–4039.
49. **Zheng, Z. L., and P. S. Stewart.** 2002. Penetration of rifampin through *Staphylococcus epidermidis* biofilms. Antimicrob. Agents Chemother. **46:**900–903.